Supplementary Experimental Procedures

Plasmids, antibodies and other reagents

The plasmids encoding Smad1 and Smad3 are described elsewhere (Sapkota et al., 2007; Sapkota et al., 2006). The linker phosphorylation site mutant forms of Smad proteins, Smad1(mut) and Smad3(mut) were previously denoted as Smad1(EPSM) (Sapkota et al., 2007), and Smad3(EPSM) (Kretzschmar et al., 1999) respectively. The YAP construct was obtained from M.B. Yaffe (MIT). pPac-Flag-Mad wild-type and linker phosphorylation mutant (S202A, 212A) were gifts from A. Laughon (University of Wisconsin). HA-Yorkie wild-type and WW domain mutant have been described in (Huang et al., 2005). For the Isothermal Titration Calorimetry experiments the region encoding the WW domains (residues 163-266) (AAH38235 entry) of human YAP was amplified by PCR and cloned into a pETM30 vector.

Total Smad1/5 antibodies were from R&D Systems (against full-length Smad1 with possible Smad5 cross-reactivity) or generated in-house (Sapkota et al., 2007). Phospho-tail Smad1/5 was phospho-Smad1(Ser463/465)/ Smad5(Ser463/465)/ Smad8(426/428) (Cell Signaling; labeled Smad1/5 due to the more restricted expression pattern of Smad8 (Arnold et al., 2006)), The Smad1/5/8 antibody (Santa Cruz Biotechnology) used in ChIP assays was also labeled Smad1/5. Smad1 pS206 (also designated pLinker) does not cross-react with Smad5 and was produced in-house (Sapkota et al., 2007). Antibodies against Smad2/3, and Smad4 were produced in-house and have been described previously (Sapkota et al., 2007) and Smad3 pS213 was from Abgent. Antibodies against Smad3 pS208 and pT179 were a gift from F. Liu (Rutgers University).

Other antibodies used were against: Smad2 phospho-tail (phospho-Smad2 (Ser465/467)), Smad2 phospho-linker (phospho-Smad2(Ser245/250/255), Smad3 phospho-tail (phospho-Smad3(Ser423/425)), p27Kip1, pRb, CDK1, CDK2, CDK4, CDK5, CDK7, CDK9, GAPDH and HA-epitope tag (all purchased from Cell Signaling); YAP and Histone 3 (Abcam); Histone 1B (Upstate Biotechnology); CDK8, Flag-HRP and α-Tubulin (Sigma-Aldrich); Flag-conjugated beads (Sigma-Aldrich); p15Ink4b (Santa Cruz Biotechnology); beta-III tubulin, tubb3 (Covance Research Products). Secondary antibodies were from Pierce.

siRNA oligonucleotide targeting *Smurf1* (Wang et al., 2003) and *FoxO4* (Seoane et al., 2004) have been described previously. Other siRNAs used in this study were: *CDK1* uggaaaccaggaagccuag; *CDK2* uccuccugggcugcaaaua; *CDK4* auuggugucggugccuaug; *CDK5* aaccgggagacucaugaga; *CDK7* gccuacauguugaugacuc; *CDK8* ggaucucuaugucggcaug; *CDK9* ccaaagcuucccccuauaa. Stable YAP knockdown in mouse ES cells was achieved using LKO1 lentiviral constructs expressing shRNA against mouse YAP (Sigma, Clone IDs: TRCN0000095864 and TRCN0000095865 were used to generate cell lines YAP#1, and YAP#2 respectively). Mouse ES cells were infected as described previously (Stewart et al., 2003).

Chromatin immunoprecipitation

Cells grown to 80% confluence were treated with or without BMP (25 nM) for 90 min and 1 h respectively. C2C12 cells were crosslinked with 1% formaldehyde for 15 min at 37^{o}C and mES cells were cross-linked with 1.6mM disuccinimidyl glutarate (Sigma) in PBS for 45 min at room temperature, followed by crosslinking with 1% formaldehyde for 15 min at room temperature. Crosslinking reactions were quenched with 0.125M glycine for 5 min at room temperature. ChIP was performed using a ChIP assay kit (Upstate Biotechnology Inc.) following the manufacturer's protocol. Immunoprecipitated DNA was analyzed by absolute qRT-PCR and the amplification product was expressed as percentage of the input for each condition. Primers used to amplify the control or promoter regions of indicated genes were: for *Id1* BRE, 5'-ccagcctgacagcccgtccgggtttta-3' (forward) and 5'-cccgggctggtctgtgtcagcgtctg-3' (reverse), described in (Komarnitsky et al., 2000{Lopez-Rovira, 2002 #64)}; for the *Id2* BRE 5'-cttgcaggcattgatcagc-3' (forward) and 5'-gagccccggagcagactc-3', predicted in (Karaulanov et al., 2004); for the *Smad7* BRE-SBE region, 5'-gggtacccctctctagacctg-3' (forward) and 5'-gtttcgcaaacaacagatcg- 3' (reverse), described in (Benchabane and Wrana, 2003) and in (Nagarajan et al., 1999; Xi et al., 2008); for the *Id1* control region, 5'-cactctgcgtggcctttc-3' (forward) and 5'-caatttagggaaggactggtttc-3' (reverse); for the *Smad7* control region, 5'-gctagctatagcatcacctctgc-3' (forward) and 5'- ctgtcaattgttttaagccttgc-3' (reverse).

Peptide synthesis

All peptides were prepared using standard Fmoc solid phase peptide synthesis with 0.1 mmol FastMoc protocols, HBTU/HOBt or HATU coupling using the Fmoc-Rink amide (Novabiochem) or Rink amide coupled ChemMatrix® (Matrix Innovation) resines. Peptides (<15 residues) were prepared in either an Applied Biosystems or in an Odyssey Microwave (CEM Corporation, Matthews, NC) peptide synthesizer. All peptides have the N-terminal amino group acetylated and an amide at the C-terminus to avoid the presence of artificial charges at both termini. Peptides were purified by reverse phase chromatography and analyzed by MALDI-TOF mass spectrometry. Neutralized peptide solutions were kept as aliquots at -20 C to prevent alkaline-induced beta-elimination of phosphate groups from phosphoserine residues. Peptide concentrations were quantified by amino acid analysis.

Isothermal titration calorimetry

Unlabeled, ^{15}N-labeled and or ^{13}C-^{15}N proteins were prepared using LB or M9 minimal media enriched with $^{15}NH_4Cl$ and with ^{13}C glucose respectively. Expression and Purification of the protein was achieved essentially as described (Macias et al., 1996). Isothermal titration calorimetry was performed using a VP-ITC MicroCalorimeter (MicroCal) at 10 °C. Protein and peptide samples were centrifuged, degassed and dissolved in the same buffer to minimize artifactual heats (100mM NaCl and 20mM deuterated tris, pH 7.5). Control determinations were done using buffer and pure peptide solutions and the heats of dilutions were subtracted from the original heats prior data analysis. Titrations were done with either the protein in the cell chamber and the PY peptide in the syringe (direct titration), or with the S206/S214/PY and pS206/pS214/PY peptides in the cell chamber and the protein in syringe. A 20x higher concentrated ligand-solution was injected (30 injections of 10 µL, at 4 min intervals) in a the cell chamber containing 1.4 mL of substrate solution. YAP polypeptide concentrations in the direct titrations varied from 20 to 200 µM depending on the affinity range expected for each complex. Concentrations of 2.0 mM were used in the reverse titrations. ITC isotherms were fit to the simplest model with MicroCal's ORIGIN software.

Supplementary References

Arnold, S.J., Maretto, S., Islam, A., Bikoff, E.K., and Robertson, E.J. (2006). Dose-dependent Smad1, Smad5 and Smad8 signaling in the early mouse embryo. Dev. Biol. *296*, 104-118.

Benchabane, H., and Wrana, J.L. (2003). GATA- and Smad1-dependent enhancers in the Smad7 gene differentially interpret bone morphogenetic protein concentrations. Mol. Cell. Biol. *23*, 6646-6661.

Blain, S.W., Montalvo, E., and Massagué, J. (1997). Differential interaction of the cyclin-dependent kinase (Cdk) inhibitor p27Kip1 with cyclin A-Cdk2 and cyclin D2-Cdk4. J. Biol. Chem. *272*, 25863-25872.

Huang, J., Wu, S., Barrera, J., Matthews, K., and Pan, D. (2005). The Hippo signaling pathway coordinately regulates cell proliferation and apoptosis by inactivating Yorkie, the Drosophila Homolog of YAP. Cell *122*, 421-434.

Karaulanov, E., Knochel, W., and Niehrs, C. (2004). Transcriptional regulation of BMP4 synexpression in transgenic Xenopus. EMBO J. *23*, 844-856.

Komarnitsky, P., Cho, E.J., and Buratowski, S. (2000). Different phosphorylated forms of RNA polymerase II and associated mRNA processing factors during transcription. Genes Dev. *14*, 2452-2460.

Kretzschmar, M., Doody, J., Timokhina, I., and Massagué, J. (1999). A mechanism of repression of TGFβ/ Smad signaling by oncogenic Ras. Genes Dev. *13*, 804-816.

Macias, M.J., Hyvonen, M., Baraldi, E., Schultz, J., Sudol, M., Saraste, M., and Oschkinat, H. (1996). Structure of the WW domain of a kinase-associated protein complexed with a proline-rich peptide. Nature *382*, 646-649.

Nagarajan, R.P., Zhang, J., Li, W., and Chen, Y. (1999). Regulation of Smad7 promoter by direct association with Smad3 and Smad4. J. Biol. Chem. *274*, 33412-33418.

Sapkota, G., Alarcón, C., Spagnoli, F.M., Brivanlou, A.H., and Massagué, J. (2007). Balancing BMP signaling through integrated inputs into the Smad1 linker. Mol. Cell *25*, 441-454.

Sapkota, G., Knockaert, M., Alarcón, C., Montalvo, E., Brivanlou, A.H., and Massagué, J. (2006). Dephosphorylation of the linker regions of Smad1 and Smad2/3 by small C-terminal domain phosphatases has distinct outcomes for bone morphogenetic protein and transforming growth factor-beta pathways. J. Biol. Chem. *281*, 40412-40419.

Seoane, J., Le, H.V., Shen, L., Anderson, S.A., and Massagué, J. (2004). Integration of Smad and forkhead pathways in the control of neuroepithelial and glioblastoma cell proliferation. Cell *117*, 211-223.

Stewart, S.A., Dykxhoorn, D.M., Palliser, D., Mizuno, H., Yu, E.Y., An, D.S., Sabatini, D.M., Chen, I.S., Hahn, W.C., Sharp, P.A.*, et al.* (2003). Lentivirus-delivered stable gene silencing by RNAi in primary cells. RNA (New York, N.Y *9*, 493-501.

Wang, H.R., Zhang, Y., Ozdamar, B., Ogunjimi, A.A., Alexandrova, E., Thomsen, G.H., and Wrana, J.L. (2003). Regulation of cell polarity and protrusion formation by targeting RhoA for degradation. Science *302*, 1775-1779.

Xi, Q., He, W., Zhang, X.H., Le, H.V., and Massagué, J. (2008). Genome-wide impact of the BRG1 SWI/SNF chromatin remodeler on the transforming growth factor beta transcriptional program. J. Biol. Chem. *283*, 1146-1155.

Figure S1. The linker regions of Smads

Schematic representation of Smad1/5 and Smad2/3 and their respective ubiquitin ligases Smurf1 and Nedd4L. Protein domains are indicated, with PY motifs within the Smad linker regions represented by green boxes. Linker phosphorylation sites are shown as colored circles: yellow, conserved (S/T)P sites; lilac, other SP sites. The WW domains of the ubiquitin ligases that are required for binding to the Smad phosphorylated linker are shown in orange. WW domain and phospho-linker interactions are indicated. Sequence alignment of the linker regions of the of the human and *Drosophila* BMP and TGFβ Smads. Phosphorylation sites are color-coded as in the schematic. The SP clusters are indicated and the PY motif is shown in green. The phosphorylation sites and PY motifs required for the interaction with Smurf1 and Nedd4L are indicated.

Figure S2. Nuclear localization of phosphorylated Smad1 and Smad2.

(A) Adjacent sections of a E13.5 mouse embryo were subjected to immunohistochemical staining using antibodies against the phosphorylated linker (site S206) and tail regions of Smad1, and Hematoxylin counterstained. Representative images of the stomach and tooth bud are shown at 40x and 80x magnification respectively. **(B)** Selected sections from the same embryo as in (A) were subjected to double-immunofluorescence staining with the same antibodies and DAPI counterstaining. In gastric and tooth bud cells, phospho-tail Smad1/5 colocalizes with phospho-linker Smad1, when the latter is present. Image magnifications were 40x for stomach and 80x for tooth bug. **(C)** Adjacent sections of a E13.5 mouse embryo, stained by immunohistochemistry with antibodies against the Smad2 phosphorylated linker and tail regions. Representative images of the tooth bud and lung are shown at 80x magnification. **(D)** Selected sections from the same embryo as in (C) were subjected to double immunofluorescence staining as in (B) with antibodies against Smad2 phopsho-linker and phospho-tail. While Smad2 phospho-tail is detected in cells surrounding the large airways and in the tooth bud, little or no Smad2 phospho-linker is detected. Images were at 80x magnification.

Figure S3. Smad4 is required for Smad1 linker phosphorylations.

The Smad4-null human pancreatic adenocarcinoma cell line BxPC3, or BxPC3 cells stably transduced with a Smad4 expression vector, were treated with BMP. Whole cell extracts were analyzed by western immunoblotting to detect the indicated proteins or phosphorylation sites.

Figure S4. Degradation of phosphorylated Smads occurs in the cytosol.

HaCaT cells were stimulated with BMP in the absence or presence of the proteasome inhibitor MG132, the CRM1 inhibitor Leptomycin B (LMB) or a combination of both. One hour post-stimulation media were replaced with fresh media without BMP. Cells were harvested at the indicated time points and nuclear and cytoplasmic fractions were analyzed by western immunoblotting to detect the indicated proteins and phosphorylation sites. α-Tubulin and Histone 1 were used as cytoplasmic and nuclear loading controls respectively.

Figure S5. Drug screening for inhibitors of linker phosphorylation.

(A, B, C, D) HaCaT cells were treated with BMP in the absence or presence of the indicated kinase inhibitors and whole cell extracts were analyzed by western immunoblotting with antibodies against the indicated proteins and phosphorylation sites.

Figure S6. Cell cycle-regulatory CDKs are not required for agonist-induced Smad linker phosphorylation

(A) Mink Lung Epithelial Mv1Lu cells harboring tetracycline-regulated p27Kip1 or p15Ink4b expression vectors (Blain et al., 1997) were grown to 80% confluency in the presence of 1 µg/ml tetracycline. The culture medium was then switched to medium without tetracycline to allow the expression of p27Kip1 and p15Ink4b. After 18 h, the cells were stimulated with BMP for 1 h and whole cell extracts were analyzed by western immunoblotting with antibodies against the indicated proteins and phosphorylation sites. **(B)** HaCaT cells were transiently transfected with siRNAs against *CDK1*, *CDK2*, *CDK4*, *CDK5*, *CDK7*, *CDK8*, *CDK9*, and the level of cognate protein knockdown was analyzed by western immunoblotting. *FoxO4* siRNA was used as a control. **(C, D)** HaCaT cells transiently transfected with siRNAs against *CDK1*, *CDK2*, *CDK4*, *CDK5*, or *FoxO4* were stimulated with BMP (C) or TGFβ (D) for 1 h and whole cell extracts were analyzed by

western immunoblotting for the presence of the indicated proteins or phosphorylation events. **(E,F)** As in (C, D) with siRNA transfection against *CDK7*, *CDK8* and *CDK9*.

Figure S7. T222 phosphorylation is not required for YAP binding to Smad1.

HEK293T cells were transfected with vectors encoding Flag-tagged Smad1 (wild-type, linker mutant or T222V point mutant). Flag immunoprecipitates were analyzed by western immunoblotting using an antibody against YAP.

Figure S8. YAP knockdown attenuates the BMP-imposed neural differentiation block in mouse ES cells.

(A) shRNA-mediated knockdown of YAP in mouse embryonic stem cells (mESCs). Mouse embryonic stem cells were lentivirally transduced with vectors encoding shRNA against YAP to generate the knockdown cell lines YAP#1 and YAP#2. YAP mRNA levels were analyzed by qRT-PCR. Data show the mean ± S.D of quadruplicates and are representative of two independent experiments. **(B)** The level of YAP knockdown in the YAP#1 and YAP#2 was analysed by western immunoblotting, together with Smad1/5 levels. Decreasing dilutions of control mESC lysate (100% to 12.5%) were tested alongside 100% of YAP#1 and YAP#2 lysates. **(C)** Confocal images of differentiating wild-type or YAP#1 knockdown mESCs. Cells were cultured in N2B27 supplemented media in the presence or absence of BMP, and five days later were subjected to immunofluorescence staining with an anti-Tubb3 antibody (green) and DAPI counterstaining (blue), to detect neuronal differentiation.

Table S1. Gene expression profiling of E14Tg2a.IV cells treated with BMP2 for one hour. Only genes whose expression is altered by ≥1.3-fold are listed. No genes were down-regulated in response to BMP when this cut-off was applied.

Gene symbol	Gene name	Fold induction by BMP2 affymetrix	Fold induction by qRT-PCR
Id3	inhibitor of DNA binding 3	3.0	2.8
Id1	inhibitor of DNA binding 1	2.9	2.9
Id4	inhibitor of DNA binding 4	2.5	2.2
Coch	coagulation factor C homolog (Limulus polyphemus)	2.0	N.D.
Zfp146	zinc finger protein 146	2.0	1.0
Smad6	MAD homolog 6 (Drosophila)	1.9	1.8
Id2	inhibitor of DNA binding 1	1.7	3.7
Sox7	SRY-box containing gene 7	1.6	N.D.
Cxcl12	chemokine (C-X-C motif) ligand 12	1.6	N.D.
Nudt21	nudix (nucleoside diphosphate linked moiety X)-type motif 21	1.5	N.D.
Smad7	MAD homolog 7 (Drosophila)	1.5	1.5
Msx2	homeo box, msh-like 2	1.4	2.5
Pitx2	paired-like homeodomain transcription factor 2	1.4	1.6
Irgm	immunity-related GTPase family, M	1.4	N.D.
Msx1	homeo box, msh-like 1	1.4	3.8
A330075 M08Rik	RIKEN cDNA A330075M08 gene	1.3	N.D.
Mid1	midline 1	1.3	1.1

Table S2. List of primers used in quantitative real-time PCR analysis of human and mouse gene transcripts.

Species	Gene name	Forward	Reverse
Human	*ID1*	aggctggatgcagttaaggg,	gacgatcgcatcttgtgtcg
	SKIL	gaggctgaatatgcaggacag	ctatcggcctcagcatgg
	CTGF	ctgcaggctagagaagcagag	gatgcacttttgcccttct
	SMAD4	tggcccaggatcagtagg	catcaacaccaattccagca
	SMAD2	tgagccacagagtaattatattccag	tgttggtcacttgtttctcca
Mouse	*Id1*	gagtctgaagtcgggaccac	gatcgtcggctggaacac
	Id2	acagaaccaggcgtccag	agctcagaagggaattcagatg
	Id3	catagactacatcctcgaccttca	cacaagttccggagtgagc
	Smad4	gagaacattggatggacgact	cacagacgggcatagatcac
	Smad6	tcctgaccagtacaagccact	ttcacccggagcagtgat
	Mid1	tgtgtgaccgatgaccagtt	tgagattactctccaagttttgctt
	Smad7	acccccatcaccttagtcg	gaaaatccattgggtatctgga
	Msx1	gccccgagaaactagatcg	ttggtcttgtgcttgcgtag
	Msx2	aggagcccggcagatact	gtttcctcagggtgcaggt
	Pixt2	gactcatttcactagccagcag	cggcgattcttgaaccaa
	Zfp146[1]	ggaaatgcctgcagtttgtt	tggaaactcagcggcttt
	GAPDH	ctccactcacggcaaattca	cgctcctggaagatggtgat
	Tubb3	ggcaactatgtaggggactcag	cctgggcacatacttgtgag
	Id4	Applied Biosystems; Taqman Assay ID: Mm00499701_m1	
	Yap1	Applied Biosystems; Taqman Assay ID: Mm00494240_m1	

[1] No intron is spanned by these primers.

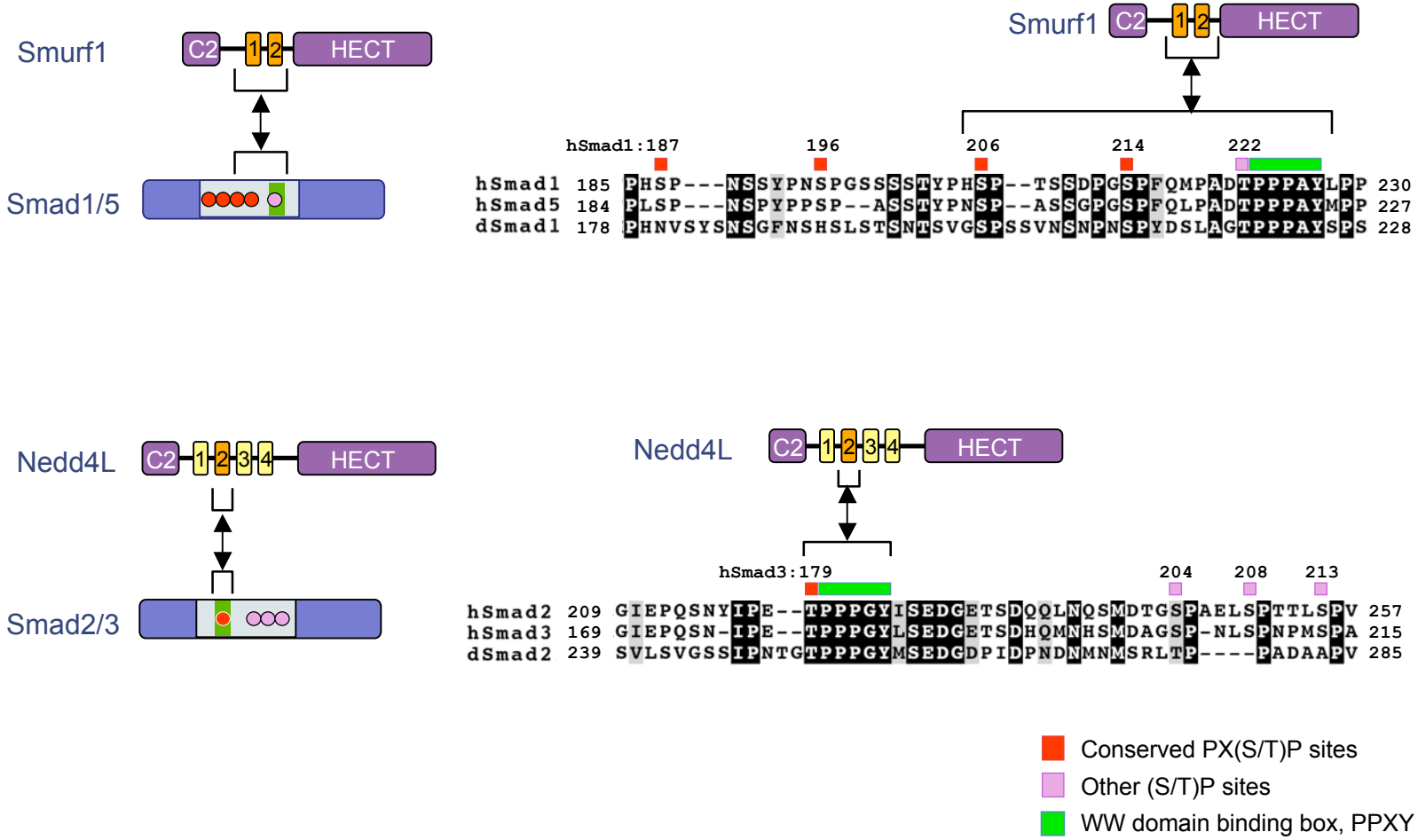

Alarcón et al Supplementary Figure 1

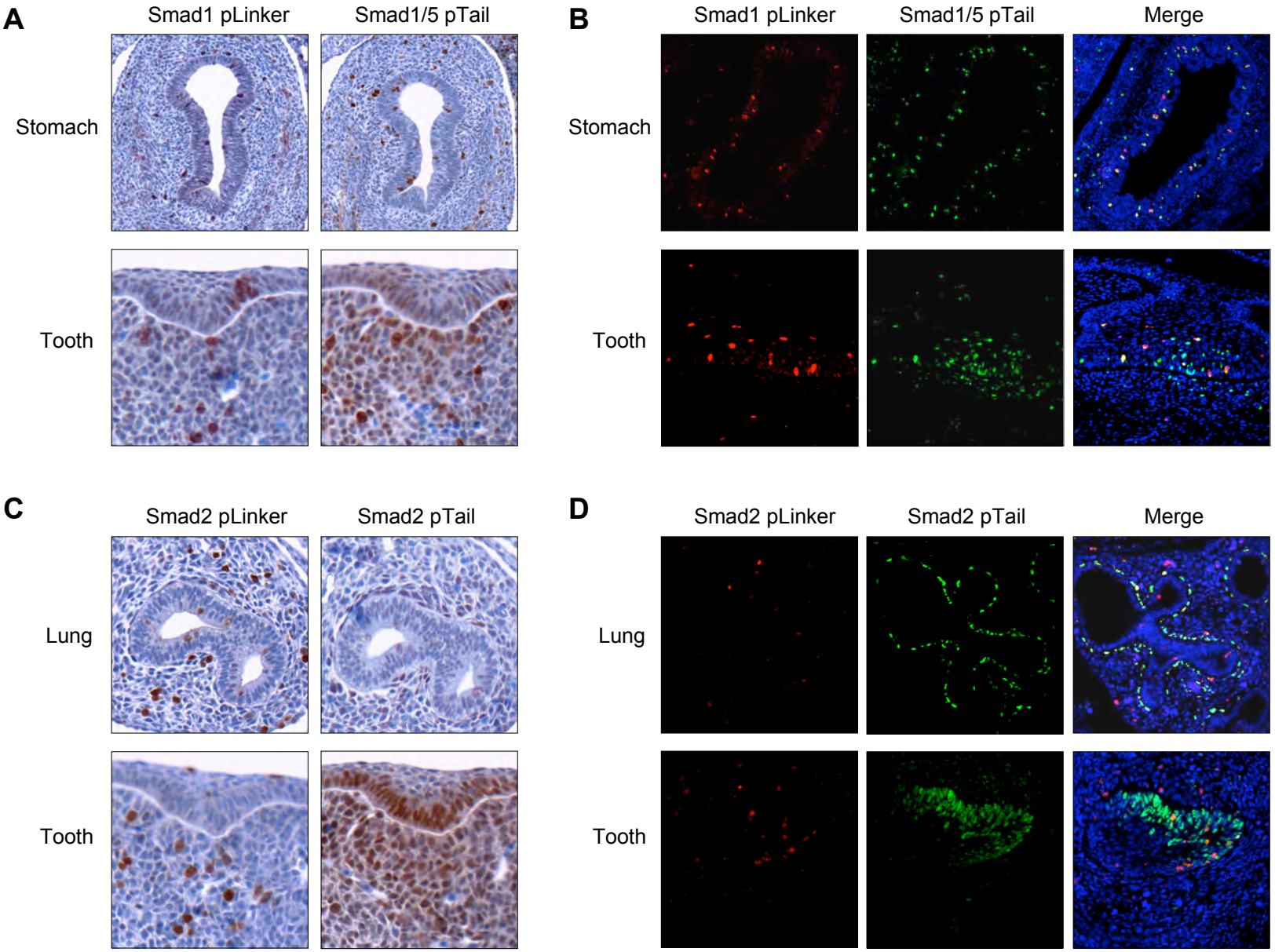

Alarcón et al Supplementary Figure 2

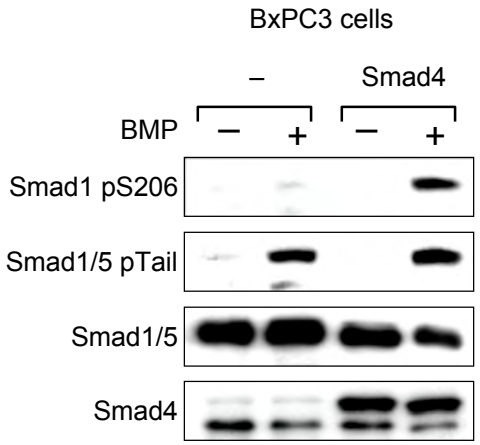
BxPC3 cells
–
Smad4
BMP
–
+
–
+
Smad1 pS206
Smad1/5 pTail
Smad1/5
Smad4

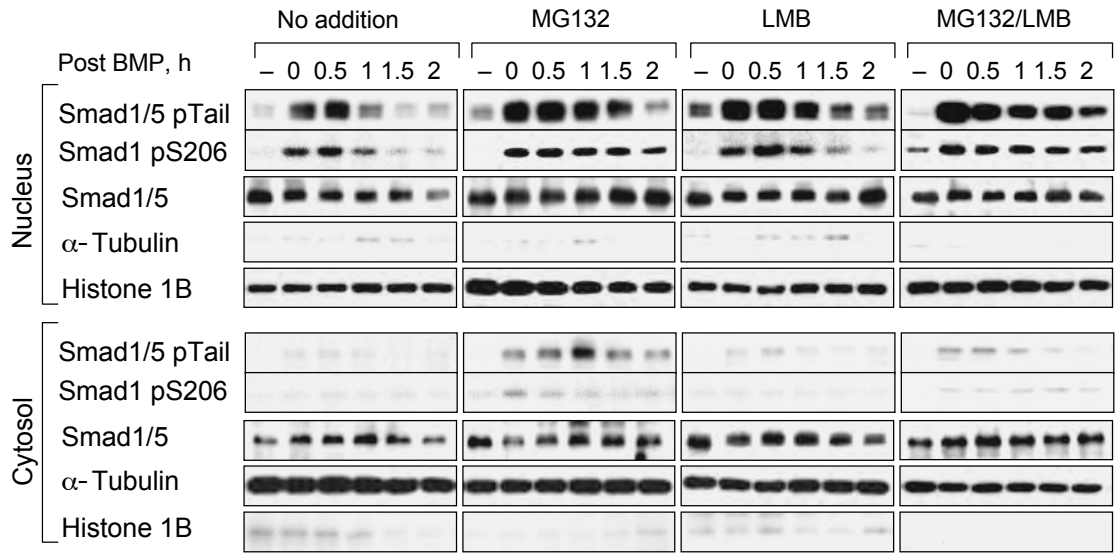

Alarcón et al Supplementary Figure 4

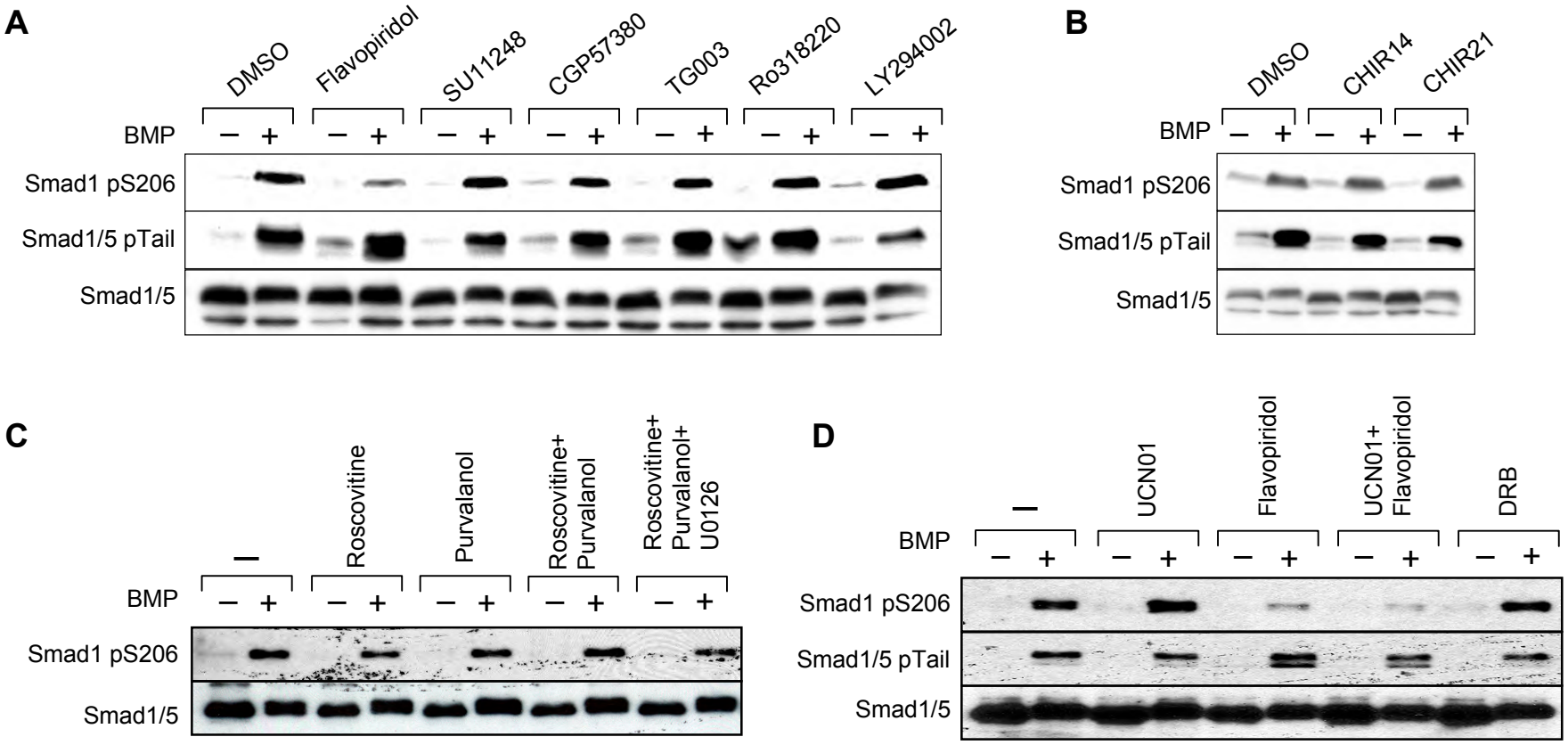
A
DMSO
Flavopiridol
SU11248
CGP57380
TG003
Ro318220
LY294002
BMP
– + – + – + – + – + – + – +
Smad1 pS206
Smad1/5 pTail
Smad1/5
B
DMSO
CHIR14
CHIR21
BMP
– + – + – +
Smad1 pS206
Smad1/5 pTail
Smad1/5
C
–
Roscovitine
Purvalanol
Roscovitine+ Purvalanol
Roscovitine+ Purvalanol+ U0126
BMP
– + – + – + – + – +
Smad1 pS206
Smad1/5
D
–
UCN01
Flavopiridol
UCN01+ Flavopiridol
DRB
BMP
– + – + – + – + – +
Smad1 pS206
Smad1/5 pTail
Smad1/5

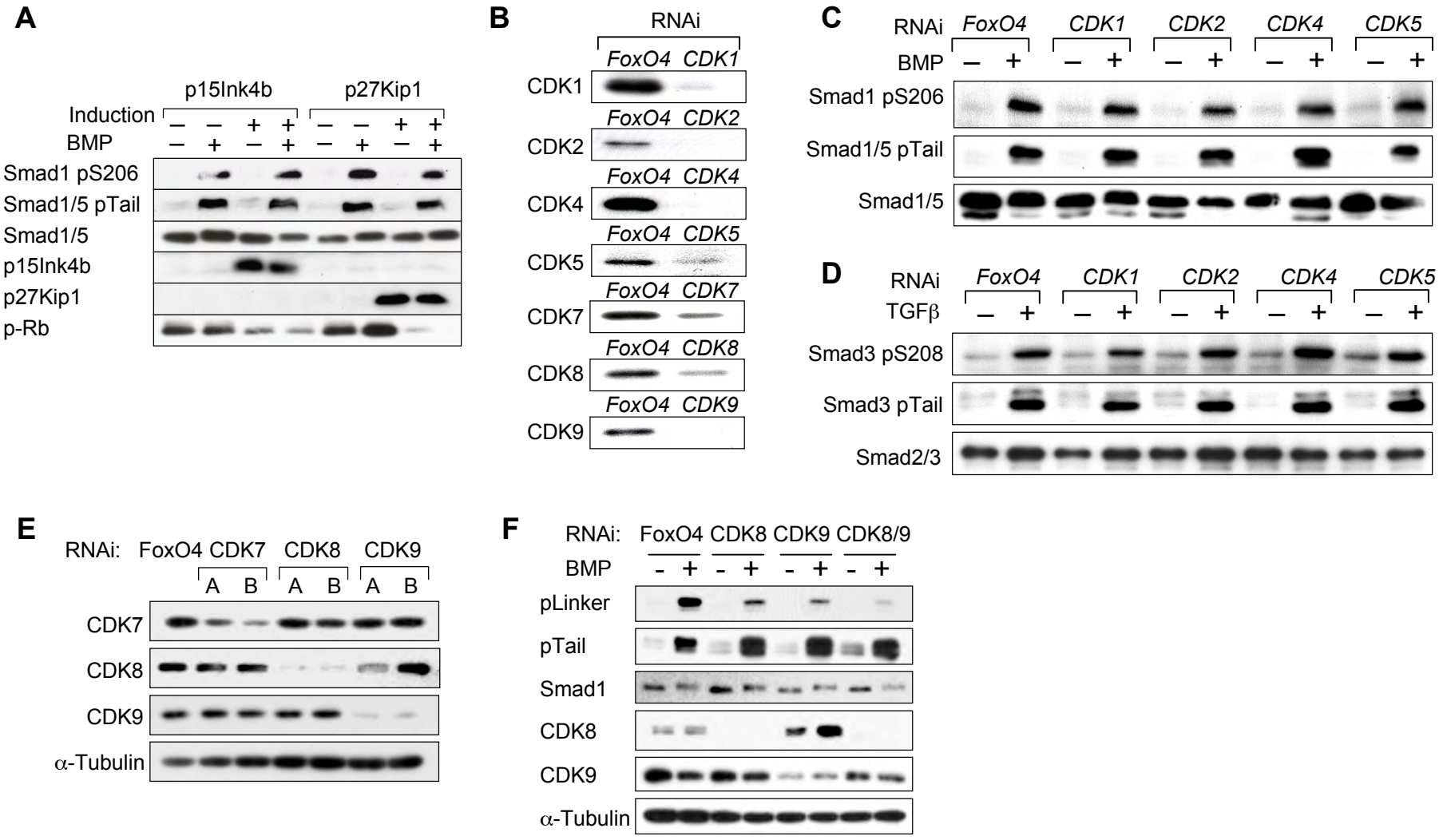

Alarcón et al Supplementary Figure 6

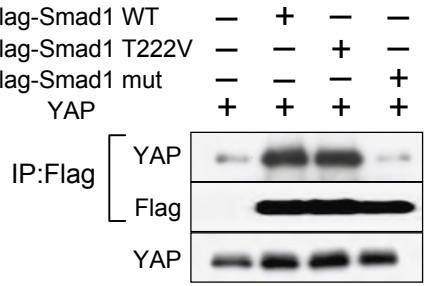
Flag-Smad1 WT
Flag-Smad1 T222V
Flag-Smad1 mut
YAP
IP:Flag
YAP
Flag
YAP

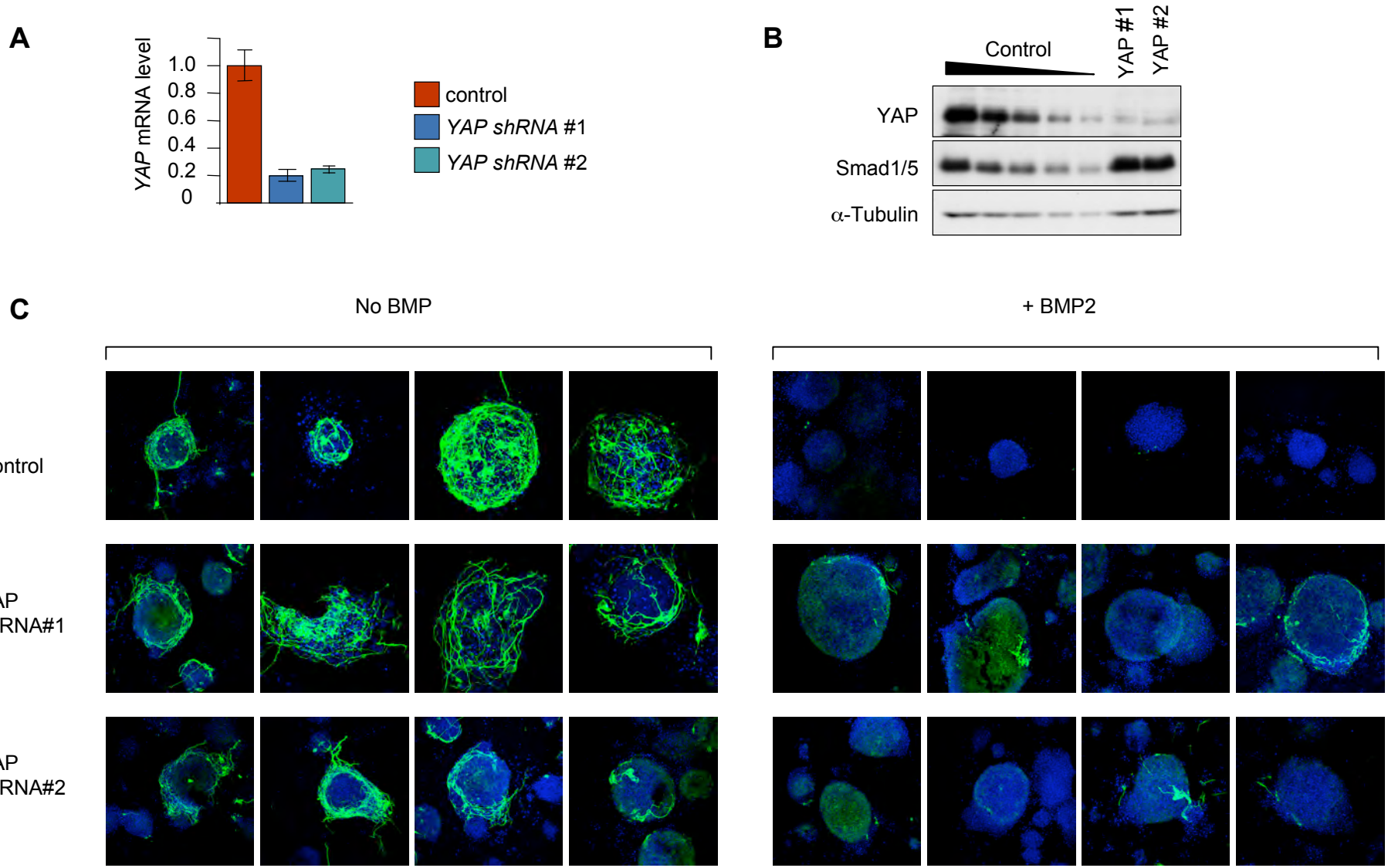
A
YAP mRNA level
1.0
0.8
0.6
0.4
0.2
0
control
YAP shRNA #1
YAP shRNA #2
B
Control
YAP #1
YAP #2
YAP
Smad1/5
α-Tubulin
C
No BMP
+ BMP2
Control
YAP shRNA#1
YAP shRNA#2